ChemComm

COMMUNICATION

View Article Online
View Journal | View Issue

Cite this: *Chem. Commun.*, 2014, **50**, 9182

Received 6th May 2014,
Accepted 26th June 2014

DOI: 10.1039/c4cc03372h

www.rsc.org/chemcomm

Synthesis of nitrogen-containing ordered mesoporous carbon as a metal-free catalyst for selective oxidation of ethylbenzene†

Jia Wang, Hongyang Liu, Xianmo Gu, Haihua Wang and Dang Sheng Su*

Nitrogen-containing ordered mesoporous carbon (NOMC) was synthesized by using *m*-aminophenol (MAP) as a carbon and nitrogen co-precursor *via* a co-assembly process with F127 in aqueous phase and exhibited a good catalytic performance for selective oxidation of ethylbenzene.

Ordered mesoporous carbon (OMC) materials have recently attracted interest because of their high specific surface areas, regular mesoporous structure and tunable pore size.[1–3] To improve their properties, surface modification is necessary and has been extensively investigated.[4] A nitrogen atom is usually induced into the carbon matrix, resulting in the improvement of surface polarity and electron-donor properties of the carbon matrix, and introduction of active basic/catalytic sites on the carbon surface.[5] Most nitrogen-containing ordered mesoporous carbon (NOMC) are synthesized through a hard-templating method using appropriate nitrogen sources,[6] such as acrylonitriles, pyrroles, anilines, melamine-formaldehyde resins and ethylenediamine-carbon tetrachloride. Although the incorporation of nitrogen into the OMC through a hard-templating method is well developed and higher nitrogen content with a C/N molar ratio of 4.3–2.3 can be achieved,[7] there is still a demand for new methods to synthesize NOMC because the hard-templating approach is low in efficiency, high in cost, has a fussy process and is harmful to health.

In recent years, an organic–organic self-assembly method has been successfully used to synthesize OMC through either a "hydrothermal"[8–10] method or an evaporation-induced self-assembly (EISA)[11–13] process. These methods provide new opportunities for the design and synthesis of OMC and heteroatom-containing OMC. Many studies have revealed that the interaction between carbon precursors and block copolymers plays a vital role in the formation of ordered mesoporous structures by the soft-templating method.[14] Therefore, the successful synthesis of NOMC through the direct soft-templating method relies much on the co-assembly of proper nitrogen-containing carbon precursors with the block co-polymer. For example, on the basis of the EISA method, Wan *et al.*[15] synthesized NOMC *via* a step-by-step method by using phenol, formaldehyde and *m*-aminophenol as an extra nitrogen source and F127 as a structure-directing agent; Zhao *et al.*[5] successfully obtained NOMC *via* self-condensation of melamine confined in the mesochannels of an OMC matrix synthesized using the EISA method; Dai *et al.*[14] demonstrated that the pyrolysis of the soft-templating polymeric composites in an ammonia atmosphere was a direct, facile way towards NOMC synthesis. Although NOMC could be synthesized according to these methods, the synthesis process is still time-consuming and is not the real direct soft-templating strategy for the synthesis of NOMC. To the best of our knowledge, there are still few reports of the direct synthesis of NOMC *via* the one-pot soft-templating method.

Herein, we selected a water-soluble *m*-aminophenol (MAP) as a carbon and nitrogen co-precursor and directly introduced N into the OMC during the co-assembly process between MAP and F127. This strategy took advantage of polymerization between MAP and formaldehyde.[16] We found that the N content of NOMC could be regulated by adding resorcinol (R) to change the molar ratio of R/MAP and changing the carbonization temperature without the loss of ordered mesoporous structure. The produced NOMC had a better catalytic activity than CMK-3 for selective oxidation of ethylbenzene.

Fig. 1 illustrates the synthesis process towards NOMC. In the first stage, MAP molecules interact with the hydrophilic PEO blocks of F127 through the hydrogen-bonding interactions, which also exist among H_2O, NH_3 and MAP. 1,3,5-Trimethylbenzene (TMB) is a non-polar molecule and is preferentially located inside the hydrophobic regions (PPO block) of F127, which easily causes the formation of stripe-like micelles.[17] During the stirring process at 80 °C, formaldehyde molecules are gradually produced by the hydrolysis of hexamine (HMT). MAP molecules undergo condensation with formaldehyde molecules forming nitrogen-containing

Shenyang National Laboratory for Materials Science, Institute of Metal Research, Chinese Academy of Sciences, 72 Wenhua road, Shenyang 110016, P. R. China. E-mail: dangsheng@fhi-berlin.mpg.de, dssu@imr.ac.cn

† Electronic supplementary information (ESI) available: Materials preparation, characterization methods, and additional figures and references. See DOI: 10.1039/c4cc03372h

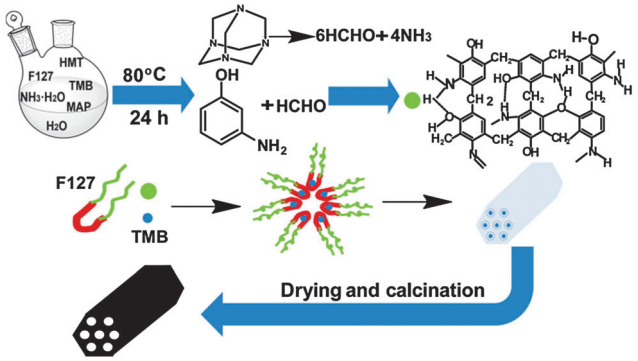

Fig. 1 Schematic representation of the synthesis route towards NOMC.

resole–F127 composites. At the same time, $-NH_2$ groups of MAP can react with the aldehyde groups *via* elimination to generate a Schiff base, which is stable because the –CH═N– bond is conjugated with a –CH═CH– bond.[15] During the calcination, most of the F127 molecules are removed below 400 °C (Fig. S1, ESI†) and the thermosetting nitrogen-containing resoles are left forming pore walls. The loss of some small molecules (such as water and NH_4^+) as well as the decomposition of functional groups due to the elevation of temperature lead to the formation of NOMC. Therefore, the basic principle relies on the polymerization of MAP and HCHO molecules around F127 to form the nitrogen-containing resole–F127 composites and the removal of F127 to obtain ordered mesoporous structures made of the nitrogen-containing pore walls after calcination. Here, for clarity, we took nitrogen-containing ordered mesoporous carbon with a molar ratio of R/MAP = 0 : 1 after carbonization at 800 °C (denoted as NOMC-800) for example, unless special instructions are given.

TEM images (Fig. 2) show that NOMC-800 has an ordered 2-D hexagonal mesoporous structure. The cell parameter, a (the distance between the two adjacent pore centres), is estimated from the TEM images to be ~12.7 nm. SEM images (Fig. S2, ESI†) of the sample indicate that the sample is composed of irregularly polyhedral particles with the size ranging from hundreds of nanometres to a few micrometres.

The ordered mesoporous structure could be further confirmed by small angle XRD analysis (Fig. 3A). The XRD pattern of NOMC-800 shows two resolved peaks at 2θ = 0.6–2.0. The ratio

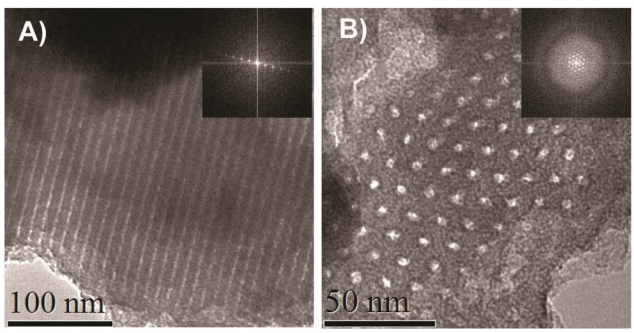

Fig. 2 TEM images of NOMC-800 with its ordered hexagonal mesoporous structure viewed from the (A) [110] and (B) [001] directions. The insets show the corresponding fast Fourier transform (FFT) patterns.

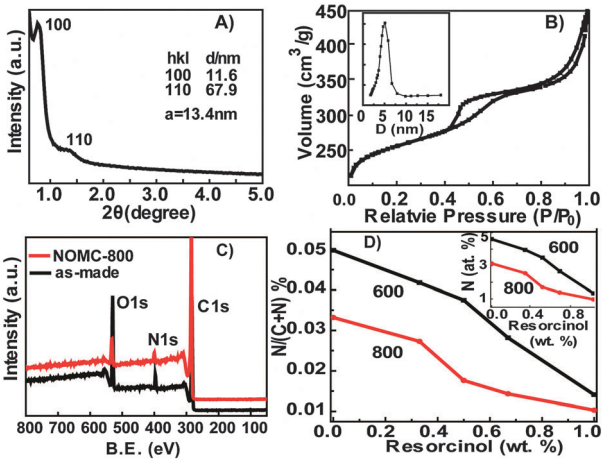

Fig. 3 (A) Small angle XRD pattern and (B) N_2 adsorption–desorption isotherms with the pore size distribution (inset) of the NOMC-800. (C) XPS spectra of the as-made and NOMC-800 and (D) the variation of the nitrogen content with the molar ratio of R/MAP and carbonization temperature.

of *d*-spacing values for these peaks is about $1 : 1/\sqrt{3}$ and can be indexed as (100) and (110) reflections associated with 2-D hexagonal *p6mm* symmetry. The cell parameter, *a*, is calculated to be ~13 nm, using the formula $a = 2d_{100}/\sqrt{3}$, where d_{100} represents the *d*-spacing value of the (100) diffraction, consistent with above TEM results. N_2 adsorption–desorption isotherms of NOMC-800 show typical type-IV curves, with a clear condensation step at P/P_0 = 0.4–0.6, suggesting a uniform mesopore (Fig. 3B). It should be noticed here that the isotherms do not give a good H1-type hysteresis loop, suggesting that some pore distortion may exist and partially block the channels.[11] According to the Brunauer–Emmett–Teller (BET) method, the specific BET surface area is calculated to be as high as 857 $m^2\ g^{-1}$. The micropore and mesopore volumes are 0.27 and 0.64 $cm^3\ g^{-1}$, respectively. The pore size calculated from the adsorption branch using the Barrett–Joyner–Halenda (BJH) model is about ~5.1 nm (see Table S1, ESI†).

XPS spectra were employed to detect the surface chemistry properties of these samples. Fig. 3C shows the spectra of NOMC-800 and the as-made sample (synthesized without carbonization, namely, nitrogen-containing resole–F127 composites) and clear signals from C, N, O of these two samples can be observed. The N content of the as-made sample is about 5.1 at%, suggesting that N can be induced into the resole–F127 composites *via* polymerization of MAP and HCHO around F127. After carbonization at 800 °C, the N content decreases to 3.3 at% and the O content decreases from 20.6 to 5.7 at% because of the decomposition of many oxygen and nitrogen functional groups and the removal of F127. Interestingly, a noticeable change in the N type is observed after carbonization at 800 °C (Fig. S3, ESI†). In the case of the as-made sample, there is one obvious peak at ~397.6 eV. After carbonization at 800 °C, the N1s peak shifts to higher binding energy, indicating an obvious change in N types which originates from rearrangement and transformation of the different N species.[18,19] The N1s spectra of NOMC-800 could be fitted to four components,

pyridinic-N (398.3 eV), pyrrolic-N (400.2 eV), graphitic-N (401.1 eV) and nitrogen-oxides (403.3 eV).[14,18,19] In order to regulate the nitrogen content, resorcinol (R) was added into the reaction system, because R was usually used to synthesize OMC.[17,20,21] The N content decreases with the rise of carbonization temperature and the molar ratio of R/MAP (Fig. 3D). For example, the N content of NOMC-800 changes from 3.3 to 0.9 at% upon tuning the weight fraction of R from 0 to 100 wt%. We propose that NH_3 from ammonia water or the hydrolysis of HMT is also partially involved in the polymerization and/or co-assembly.[22] Therefore, there is still some N remaining when only R is used. Nevertheless, the main source of N comes from MAP molecules (Fig. S4, ESI†). Alternatively, small XRD patterns (Fig. S5, ESI†), N_2 adsorption–desorption isotherms (Fig. S6, ESI†), TEM images (Fig. S7 and S9, ESI†) and XPS characterization data (Fig. S8 and S10, ESI†) of other products given in the ESI† also confirm that we successfully synthesized NOMC with a tunable N content.

NOMC has been used in adsorption, separation, and energy storage/conversion, but there are few reports of NOMC as a metal-free catalyst.[4,23] It has been demonstrated that N in N-doped graphene plays a vital role in the C–H activation.[24] This progress encouraged us to test the produced NOMC in selective liquid-phase oxidation of ethylbenzene. The results of various carbon catalysts are summarized in Table 1. In our experiment, acetophenone (AcPO) is the main product with benzaldehyde, benzoic acid and 1-phenyl-ethylalcohol as the by-products, which is in line with CNTs and/or N-doped graphene as catalysts.[24,25] The blank test indicates that there is a low reaction activity because of the EB autoxidation.[26] CMK-3 exhibits higher catalytic performance than that observed in the blank test, indicating that the mesoporous carbon material itself has a certain catalytic ability for the formation of AcPO. However, O-CMK-3 (CMK-3 treated with HNO_3) has a lower activity than CMK-3, which may be attributed to the side-effects of oxygen-functional groups introduced *via* HNO_3-treatment.[25,27] There is an obvious increase of catalytic performance when NOMC-800 is used as a catalyst. We propose that N introduced into the OMC plays a very important role in the reaction, which is in agreement with a previous report.[24] Moreover, although NOMC prepared *via* a similar literature method[14] exhibits approximate activity (see properties of NH_3-OMC-800 in Table S2, ESI†), in the view of the synthesis process, NOMC-800 prepared in this work has an advantage over the NH_3 treatment. It is worth noting that no metal is induced into the material which is very important for the carbon catalysis research to exclude the effects of the metal impurities in the carbon catalyst.[28]

Table 1 Catalytic activity of different carbon materials for the liquid phase oxidation of ethylbenzene[a]

Sample	Conversion (%)	Selectivity (%)	R_s[b] (μmol m^{-2} h^{-1})
Blank	13.8	14.1	—
CMK-3	40.8	40.2	40.8
O-CMK-3[c]	34.9	30.7	39.1
NOMC-800	63.3	84.1	168.7
NH_3-OMC-800	63.1	86.1	108.1

[a] The conversion and selectivity for (AcPO) were determined by GC. [b] Yield rate of AcPO per m^2 of the catalyst surface at 12 h. [c] CMK-3 is treated with concentrated HNO_3 for 3 h, at 60 °C and denoted as O-CMK-3.

In conclusion, using MAP as a carbon and nitrogen co-precursor, nitrogen-containing ordered mesoporous carbon has been successfully synthesized *via* a co-assembly process between MAP and F127. Our results show that this approach is simpler for direct introduction of nitrogen into the OMC compared with traditional NH_3 post-treatment, step-by-step strategies and other hard-templating methods. Furthermore, this work enlarges the application of OMC in catalysis especially by using OMC as a metal-free catalyst.

This work was supported by the National Natural Science Foundation of China (21203214, 21133010, 51221264, and 21261160487), MOST (2011CBA00504), the ''Strategic Priority Research Program'' of the Chinese Academy of Sciences (Grant No. XDA09030103), and the China Postdoctoral Science Foundation (2012M520652). Dr Zhenhua Sun is gratefully acknowledged for his stimulating discussions.

Notes and references

1 T. Y. Ma, L. Liu and Z. Y. Yuan, *Chem. Soc. Rev.*, 2013, **42**, 3977.
2 C. Liang, Z. Li and S. Dai, *Angew. Chem., Int. Ed.*, 2008, **47**, 3696.
3 J. Lee, J. Kim and T. Hyeon, *Adv. Mater.*, 2006, **18**, 2073.
4 W. Z. Shen and W. B. Fan, *J. Mater. Chem. A*, 2013, **1**, 999.
5 Z. Wu, P. A. Webley and D. Y. Zhao, *J. Mater. Chem.*, 2012, **22**, 11379.
6 (*a*) A. H. Lu, A. Kiefer, W. Schmidt and F. Schüth, *Chem. Mater.*, 2004, **16**, 100; (*b*) C. M. Yang, C. Weidenthaler, B. Spliethoff, M. Mayanna and F. Schüth, *Chem. Mater.*, 2005, **17**, 355; (*c*) A. Vinu, S. Anandan, C. Anand, P. Srinivasu, K. Ariga and T. Mori, *Microporous Mesoporous Mater.*, 2008, **109**, 398; (*d*) W. R. Li, D. H. Chen, Z. Li, Y. F. Shi, Y. Wan, G. Wang, Z. Y. Jiang and D. Y. Zhao, *Carbon*, 2007, **45**, 1757; (*e*) A. Vinu, P. Srinivasu, D. P. Sawant, T. Mori, K. Ariga, J. S. Chang, S. H. Jhung, V. V. Balasubramanian and Y. K. Hwang, *Chem. Mater.*, 2007, **19**, 4367.
7 A. Vinu, K. Ariga, T. Mori, T. Nakanishi, S. Hishita, D. Golberg and Y. Bando, *Adv. Mater.*, 2005, **17**, 1648.
8 D. Liu, J. H. Lei, L. P. Guo and K. J. Deng, *Carbon*, 2011, **49**, 2113.
9 L. Liu, F. Y. Wang, G. S. Shao and Z. Y. Yuan, *Carbon*, 2010, **48**, 2089.
10 Y. Huang, H. Cai, D. Feng, D. Gu, Y. Deng, B. Tu, H. Wang, P. A. Webley and D. Zhao, *Chem. Commun.*, 2008, 2641.
11 Y. Meng, D. Gu and D. Y. Zhao, *Chem. Mater.*, 2006, **18**, 4447.
12 C. F. Xue, B. Tu and D. Y. Zhao, *Adv. Funct. Mater.*, 2008, **18**, 3914.
13 M. Florent, C. Xue, D. Zhao and D. Goldfarb, *Chem. Mater.*, 2012, **24**, 383.
14 X. Wang, C. G. Liu, D. Neff, P. F. Fulvio, R. T. Mayes, A. Zhamu, Q. Fang, G. Chen, H. M. Meyer, B. Z. Jang and S. Dai, *J. Mater. Chem. A*, 2013, **1**, 7920.
15 C. Feng, H. Li and Y. Wan, *J. Nanosci. Nanotechnol.*, 2009, **9**, 1558.
16 J. Zhao, W. Niu, L. Zhang, H. Cai, M. Han, Y. Yuan, S. Majeed, S. Anjum and G. Xu, *Macromolecules*, 2013, **46**, 140.
17 D. Liu, J. H. Lei, L. P. Guo, D. Qu, Y. Li and B. L. Su, *Carbon*, 2012, **50**, 476.
18 R. Arrigo, M. Havecker, R. Schlogl and D. S. Su, *Chem. Commun.*, 2008, **40**, 4891.
19 S. Kundu, W. Xia, W. Busser, M. Becker, D. A. Schmidt, M. Havenith and M. Muhler, *Phys. Chem. Chem. Phys.*, 2010, **12**, 4351.
20 X. Q. Wang, C. D. Liang and S. Dai, *Langmuir*, 2008, **24**, 7500.
21 A. H. Lu, B. Spliethoff and F. Schuth, *Chem. Mater.*, 2008, **20**, 5314.
22 L. Liu, Q. F. Deng, X. X. Hou and Z. Y. Yuan, *J. Mater. Chem.*, 2012, **22**, 15540.
23 K. Kwon, Y. J. Sa, J. Y. Cheon and S. H. Joo, *Langmuir*, 2012, **28**, 991.
24 Y. Gao, G. Hu, J. Zhong, Z. Shi, Y. Zhu, D. S. Su, J. Wang, X. Bao and D. Ma, *Angew. Chem., Int. Ed.*, 2013, **52**, 2109.
25 J. Luo, F. Peng, H. Yu, H. Wang and W. Zheng, *ChemCatChem*, 2013, **5**, 1578.
26 I. Hermans, J. Peeters and P. A. Jacobs, *J. Org. Chem.*, 2007, **72**, 3057.
27 H. Yu, F. Peng, J. Tan, X. W. Hu, H. J. Wang, J. Yang and W. X. Zheng, *Angew. Chem., Int. Ed.*, 2011, **123**, 4064.
28 J. Zhang, X. Liu, R. Blume, A. Zhang, R. Schlogl and D. S. Su, *Science*, 2008, **322**, 73.

